

Effect of Surface Hydrophobicity on the Function of the Immobilized Biomineralization Protein Mms6

Xunpei Liu,^{†,‡,+} Honghu Zhang,^{†,§,+} Srikanth Nayak,^{†,‡} German Parada,[‡] James Anderegg,[†] Shuren Feng,^{†,||} Marit Nilsen-Hamilton,^{†,||} Mufit Akinc,^{†,§} and Surya K. Mallapragada^{*,†,‡}

[†]Division of Materials Science and Engineering, Ames Laboratory, Ames, Iowa 50011, United States

[‡]Department of Chemical & Biological Engineering, [§]Department of Materials Science & Engineering, and ^{||}Roy J. Carver Department of Biochemistry, Biophysics and Molecular Biology, Iowa State University, Ames, Iowa 50011, United States

Supporting Information

ABSTRACT: Magnetotactic bacteria produce magnetic nanocrystals with uniform shapes and sizes in nature, which has inspired in vitro synthesis of uniformly sized magnetite nanocrystals under mild conditions. Mms6, a biomineralization protein from magnetotactic bacteria with a hydrophobic N-terminal domain and a hydrophilic C-terminal domain, can promote formation of magnetite nanocrystals in vitro with well-defined shape and size in gels under mild conditions. Here we investigate the role of surface hydrophobicity on the ability of Mms6 to template magnetite nanoparticle formation on surfaces. Our results confirmed that Mms6 can form a protein network structure on a monolayer of hydrophobic octadecanethiol (ODT)-coated gold surfaces and facilitate magnetite nanocrystal formation with uniform sizes close to those seen in nature, in contrast to its behavior on more hydrophilic surfaces. We propose that this hydrophobicity effect might be due to the amphiphilic nature of the Mms6 protein and its tendency to incorporate the hydrophobic N-terminal domain into the hydrophobic lipid bilayer environment of the magnetosome membrane, exposing the hydrophilic C-terminal domain that promotes biomineralization. Supporting this hypothesis, the larger and well-formed magnetite nanoparticles were found to be preferentially located on ODT surfaces covered with Mms6 as compared to control samples, as characterized by scanning electron microscopy, X-ray diffraction, X-ray photoelectron spectroscopy, and atomic force microscopy studies. A C-terminal domain mutant of this protein did not form the same network structure as wild-type Mms6, suggesting that the network structure is important for the magnetite nanocrystal formation. This study provides valuable insights into the role of surface hydrophilicity on the action of the biomineralization protein Mms6 to synthesize magnetic nanocrystals and provides a facile route to controlling bioinspired nanocrystal synthesis in vitro.

INTRODUCTION

Magnetic nanoparticles exhibit many interesting properties that can be exploited in a variety of applications such as catalysis, biomedicine, quantum computing, and data storage.^{1–4} Magnetic nanoparticles can be synthesized using sol–gel methods, high-pressure hydrothermal methods, liquid phase coprecipitation, gas phase thermal decomposition, etc.^{1–6} However, these methods usually require high temperature treatments^{6,7} or cannot generate nanoparticles with uniform size and shape, which can potentially limit their applications.⁸ In nature, magnetotactic bacteria produce magnetic nanocrystals under mild conditions and have high chemical purity, narrow size ranges, and species-specific crystal morphologies.^{9–11} These nanocrystals, usually magnetite (Fe_3O_4) or greigite (Fe_3S_4), are surrounded by a lipid bilayer membrane about 3–4 nm thick to form the unique intracellular structures called magnetosomes.^{9,10} Using these aligned nanocrystals, the magnetotactic bacteria can orient themselves and navigate along geomagnetic field lines.^{12,13} Although magnetotactic bacteria were discovered almost four decades ago, little is known about the mechanisms by which bacteria synthesize these magnetic crystals.^{9,11,14} Recently, with the discovery and isolation of new bacterial strains and the development of new techniques, there has been progress in understanding magnetosome formation.^{9,15,16} Inspired by nature, the chemical

synthesis of hybrid materials with unusual morphologies at several length scales has received considerable interest from the research community.^{17,18} Bioinspired in vitro synthetic routes offer room-temperature pathways for the production of a variety of hybrid magnetic nanostructures with exceptional control over nanoparticle nucleation and growth and are expected to ultimately enable the fabrication of structurally perfect and functional hierarchical systems with sizes, shapes, and properties not easily realizable via conventional synthetic techniques under mild conditions.¹⁹ Synthesis of magnetic nanomaterials using magnetotactic bacteria *in vivo* or related proteins *in vitro* has progressed quickly.^{19,20} However, the role of surface hydrophobicity on the action of biomineralization proteins has not been well-studied and could have significant implications in bioinspired nanocrystal synthesis.

Mms6 is a biomineralization protein found associated with the magnetite nanocrystals inside the magnetosomes of *Magnetospirillum magneticum* AMB-1, which promotes the

Special Issue: Doraiswami Ramkrishna Festschrift

Received: April 15, 2015

Revised: July 11, 2015

Accepted: August 13, 2015

Published: August 13, 2015



formation of superparamagnetic magnetite nanocrystals under room temperature and mild conditions *in vitro*.^{21–25} Mms6 is an amphiphilic protein with a hydrophobic N-terminal domain and a hydrophilic C-terminal domain. The protein self-assembles into micelles in solution and the C-terminus can bind iron with very high affinity.²⁵ The interaction between Mms6 and iron is believed to be the initial step of biominerization,^{25–27} and several mutants were synthesized to investigate the biominerization mechanism. For instance, in a mutant m2Mms6, the hydrophilic C-terminal domain of the protein was altered such that the amino acid residues containing hydroxyl or carboxyl groups are shuffled with respect to one another, still maintaining the same hydrophathy plot as Mms6.^{25,28} Compared with Mms6, m2Mms6 does not bind iron.^{22,25} Recently, magnetite nanoparticles were synthesized with Mms6 on planar substrates by bottom-up approaches, in which Mms6 immobilized on surfaces provided interaction sites with irons and initiated magnetite formation.^{29–31} The nonspecific binding of Mms6 to the octadecyltrimethoxysilane monolayer on a silicon substrate results in formation of multiple layers of iron oxide nanoparticles.²⁹ Mms6 has also been chemically immobilized onto surfaces by soft-lithography to promote magnetite nanoparticles' growth on surfaces, which could be potentially used for high density data storage.³⁰ This chemical immobilization was achieved by using *N*-hydroxysuccinimide (NHS)/ethyl-(dimethylaminopropyl) (EDC) chemistry to attach the amine groups in the protein to the carboxyl group on the surface. However, there are 13 amine groups in an Mms6 molecule, and nonspecific linkage reactions could alter the structure or function of Mms6.^{30,31}

As Mms6 is an amphiphilic membrane protein, and is believed to be embedded in the phosphate lipid bilayer membrane in bacteria, in this study, we physically incorporated Mms6 onto surfaces with different hydrophobicities without covalent linkages. This allowed us to investigate the role of surface hydrophilicity on Mms6 structure and function. Three different kinds of surfaces were used: hydrophobic 1-octadecanethiol (ODT), gold, and a relatively hydrophilic poly(ethylene glycol) surface. Mms6 was coated on these surfaces to study its ability to promote magnetite nanocrystal growth.

MATERIALS AND METHODS

Materials. Mms6 and its mutant m2Mms6 were prepared and purified as reported before.^{25,28,32} m2Mms6 includes the same sequence as Mms6 in the N-terminal (hydrophobic) domain and an altered sequence in the C-terminal (hydrophilic) domain. The hydroxyl/carboxyl containing amino acid residues in the C-terminal domain are shuffled with respect to wild-type Mms6. Compared with Mms6, m2Mms6 does not bind iron.^{22,25} The m2Mms6 and Mms6 used in this study were expressed with an N-terminal poly histidine tag (His-tag). For simplicity, the His-tagged Mms6 or m2Mms6 are referred to here as Mms6 or m2Mms6. Mms6 consists of 133 amino acid residues, is ~10 kDa with a calculated molecular volume of $\sim 1.3 \times 10^4 \text{ \AA}^3$. The Mms6 solution used in this study was 0.2 mg/mL in 20 mM Tris buffer with 100 mM KCl (pH 7.5).

1-Octadecanethiol (ODT) and lysozyme were purchased from Sigma-Aldrich. Poly(ethylene glycol) methyl ether thiol (henceforth referred to as PEG) (average $M_n = 2000$) was purchased from NOF America corporation. Iron(III) chloride hexahydrate ($\text{FeCl}_3 \cdot 6\text{H}_2\text{O}$, ≥98%), iron(II) chloride tetrahy-

drate ($\text{FeCl}_2 \cdot 4\text{H}_2\text{O}$, 99.99%), and Pluronic F-127 were purchased from Sigma-Aldrich, and potassium chloride (KCl, ≥99%) and tris base (≥99.8%) were purchased from Fisher Scientific. All chemicals were used without further purification. ODT or PEG were dissolved in ethanol to make a 2 mM solution. Both solutions were freshly made and sonicated for 5 min to dissolve the solute. FeCl_3 and FeCl_2 stock solutions were degassed and purged with inert gas (nitrogen or argon) prior to use.

Surface Preparation. All the surface samples were prepared on 1 cm × 1 cm square glass microscope slides, and the flat gold surfaces were obtained by a template-stripping method.³³ Briefly, template-stripped gold was prepared by resistively evaporating about 250 nm of gold onto a 4-in. silicon wafer with an Edwards 306A resistive evaporator. Glass microscope slides were cut into 1 cm × 1 cm squares and sonicated in diluted 5% Contrad 70 liquid detergent, deionized water, and ethanol (twice), each for 30 min, and dried under a nitrogen stream. The clean glass substrates were glued to the gold-coated wafer with two-part epotek 377 (Epoxy Technology) and heated at 150 °C for 1.75 h. The glass substrates were then gently detached from the silicon wafer. The sandwiched gold film remained on the topside of the glass substrate to yield a smooth gold surface. The process is shown schematically in Figure 1A.

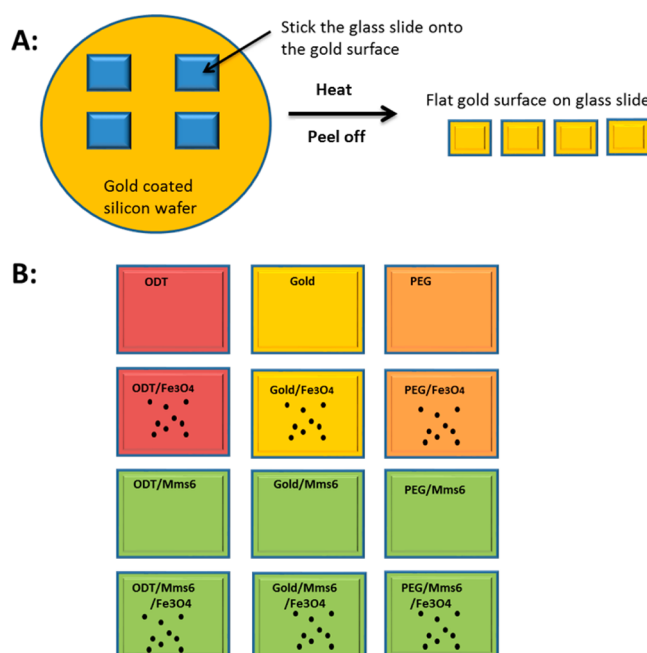


Figure 1. Schematic representation of sample preparation steps: (A) gold surface fabrication; (B) experiment design and characterization.

The smooth gold surface was dipped into 2 mM ODT or PEG solution in a small glass dish and was incubated overnight at room temperature to create a self-assembled monolayer of ODT or PEG. The surface was then dried by nitrogen flow. The ODT or PEG coated gold surface is referred to as ODT surface or PEG surface henceforth, as shown schematically in the first row of Figure 1B.

A 30 μL portion of 0.2 mg/mL Mms6 in Tris buffer was added to the gold or ODT or PEG surface and incubated overnight in a humidity chamber at 4 °C. The surface was then washed in Tris buffer and water with 0.5% Tween 20 and dried

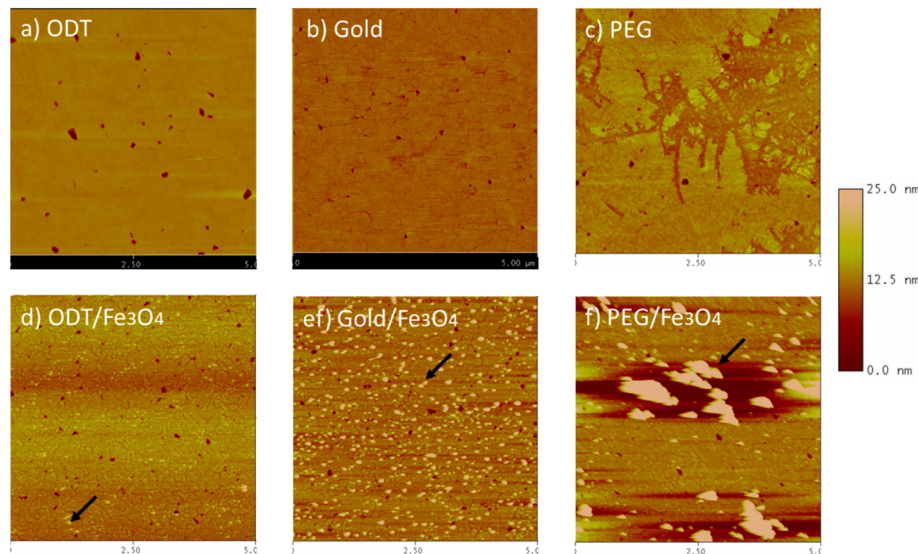


Figure 2. AFM scans of surfaces without Mms6 before magnetite nanoparticles synthesized on (a) ODT, (b) gold, and (c) PEG surfaces; and after synthesis of magnetite nanoparticles (d) magnetite grown on ODT surface, (e) magnetite grown on gold surface, and (f) magnetite grown on PEG surface. Arrows are used to highlight particles on surfaces. Scan area $5\text{ }\mu\text{m} \times 5\text{ }\mu\text{m}$.

under nitrogen stream for tests. The drying step here was skipped for the Mms6-coated surface used for the magnetite formation. The surfaces are referred to as ODT/Mms6, gold/Mms6, and PEG/Mms6, as shown in Figure 1B on the third row.

Magnetite Growth on the Surfaces. Magnetite nanoparticles were grown on the surfaces by a coprecipitation method. The method was developed based on our previous bulk solution synthesis of magnetite nanoparticles.^{22,25} All solutions used in the following procedures were prepared using degassed water. Briefly, a stock solution with polymer and iron ions was prepared at $4\text{ }^{\circ}\text{C}$ using the following ratio: $100\text{ }\mu\text{L}$ of 25 wt \% Pluronic F127 solution, $50\text{ }\mu\text{L}$ of 0.25 M FeCl_2 solution, $50\text{ }\mu\text{L}$ of 0.5 M FeCl_3 solution, and $100\text{ }\mu\text{L}$ of Tris buffer. In a glovebox charged with inert gas (nitrogen or argon), glass substrates treated with ODT/PEG and Mms6 were added to wells in a 24-well plate. A $200\text{ }\mu\text{L}$ portion of the stock solution containing polymer and iron ions was brought up to room temperature, slowly added to each well by micropipette, and incubated for 2 h at room temperature without controlling the humidity. Then $750\text{ }\mu\text{L}$ of 0.1 M NaOH solution was slowly added to each well, and all the samples were incubated under an oxygen free environment for 5 days . The surface samples were then washed three times using degassed water and sealed under nitrogen gas until subsequent characterization tests. The black precipitate in the suspension was collected and washed for powder X-ray diffraction (XRD) characterization. The surface samples with magnetite nanoparticles are shown schematically in Figure 1B in rows 2 and 4.

Measurements. Atomic force microscopy (AFM) topographic images were acquired using a Nanoscope III Digital Instruments AFM (Veeco) in tapping mode. XRD analysis of the powders was performed using a PANalytical X'Pert Pro diffraction system equipped X'pert Data collector in which a cobalt $\text{K}\alpha$ radiation source with a wavelength of 0.17903 nm was employed. Formation of magnetite nanoparticles on surfaces was examined with scanning electron microscopy (SEM, FEI Quanta 250). Magnetic force microscopy (MFM) images were obtained using MESP (Bruker) at the Center for

Nanoscale Materials at the Argonne National Lab. X-ray photoelectron spectroscopy (XPS) surface analysis was performed with a PHI 5500 spectrometer using $\text{Al}-\text{K}\alpha 1$ radiation with a 45° electron collection angle, corresponding to the maximal penetration depth of about 10 nm . For contact angle measurements, $2\text{ }\mu\text{L}$ of nanopure water was dropped on the surface of interest, and the drops were photographed with Canon EOS Rebel T3i EF 100 mm f/2.8L Macro IS USM. The half angle method was used to obtain the contact angles.

RESULTS AND DISCUSSION

The gold surface obtained by the template stripped method was very flat, as shown in Figure 2b. The roughness of the gold surface was about $2\text{--}3\text{ nm}$, determined by the line cross-sectional view of the AFM images. Such a flat surface provided the ability to image the nanoparticles on the surface. Self-assembled monolayers of ODT or surfaces covered with PEG were formed on the flat gold surfaces after overnight incubation. The ODT surface is hydrophobic,³⁴ and the PEG surface is hydrophilic,³⁵ as observed during Mms6 incubation, which is verified by the contact angle measurements, shown in Figure 3. There were no obvious differences seen in the images between the ODT and gold surfaces (Figure 2a and b), since the alkyl chains from *n*-alkanethiols prefer a parallel alignment on the gold surface and formation of a close-packed monolayer with the ellipsometric thickness of about 2 nm for ODT.³⁴ However, PEG did not uniformly cover the gold surface (Figure 2c). In a self-assembled monolayer, the PEG chain is not “extended”, but rather folds on itself sometimes.^{35,36} Unlike the “brush” conformation of ODT on gold, PEG chains sometimes arrange in “island” or “mushroom” conformations.^{37,38} In addition, the PEG used in this study had a much larger molecular weight ($M_n = 2000$) than ODT ($M_w = 286.56$), indicating that PEG had longer, disorganized chains, which might further prevent the formation of a uniform and dense monolayer.^{35,36}

Magnetite nanoparticles were synthesized by the coprecipitation method on ODT, PEG, and bare gold surfaces. Assuming that magnetite nanoparticles do not interact strongly with

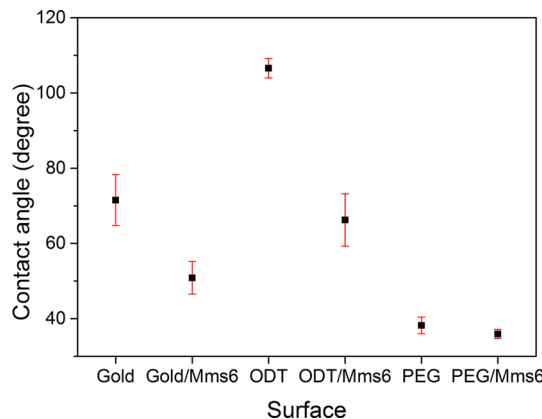


Figure 3. Contact angles for gold, ODT, and PEG surfaces with and without Mms6 coating.

ODT, PEG, and gold surfaces, in the absence of Mms6 there should be no magnetite nanoparticles left on the surface after the washing process. However, the images show that there were a few residual magnetite nanoparticles and aggregates left on the surface even after washing process (Figure 2d–f), implying that it was difficult to completely wash off the magnetite particles even from the perfectly smooth surfaces with just the water flow. The lighter spots (see arrows) in the AFM images in Figure 2d–f correspond to areas with greater height, corresponding to the presence of the magnetite nanoparticles. It is also possible that, during washing process at neutral pH, the negatively charged gold surface might attract slightly positively charged magnetite particles, since the isoelectric points (IEPs) of gold and magnetite nanoparticles are around 2.5 and 8, respectively, as reported previously.^{39,40}

Mms6 was coated on ODT, PEG, and bare gold surfaces (Figures 4a–c and S1a–c). On the gold surface, Mms6 formed spherical nanomicellar structures. This is consistent with previous observations that Mms6 self-assembles to form micelles in solution,^{25,28} which explains the micellar structure formation on the gold surface probably due to adsorption.

Mms6 showed very different morphology on the ODT surface than on the gold surface. As can be seen from Figures 4a and S1a, Mms6 formed larger self-assembled units that resemble a connected protein network. However, there were no obvious significant differences between Mms6 on the PEG surface and for PEG alone, as seen in Figures 2c, 4c, and S1c. This may be caused by the well-known protein resistant property of the PEG.⁴¹ Contact angle measurements done on these surfaces after Mms6 incubation (Figure 3) also indicate protein coated on the gold and ODT surfaces as opposed to the PEG surface. After Mms6 coating, the contact angles of the gold and ODT surfaces decreased by 10–30° and 30–50°, respectively, while no change of contact angle was observed on the PEG surface.

Figures 4d–f and S1d–f show the magnetite nanoparticles grown on the Mms6 coated surfaces. Comparing with Figures 2d–f, there were significantly more magnetite nanoparticles seen on ODT and gold surfaces with Mms6 than without, while magnetite nanoparticles grown on PEG surface with and without Mms6 looked similar. This suggests that Mms6 remained on the ODT and gold surfaces and not the PEG and, in that form, could promote the formation of magnetite nanoparticles on surfaces, similar to what is seen in bulk solution.^{22,25} The collected black precipitates from the solution during synthesis of magnetite on Mms6 coated ODT surface were also confirmed as magnetite by XRD (Figure S2). In the presence of Mms6, magnetite nanoparticles were uniformly distributed on the ODT surface without formation of the aggregates as were seen on the gold surface. The particles on the ODT surfaces were larger than those on gold, with a size of about 20 nm, which is close to the size of the magnetite nanocrystals generated by magnetotactic bacteria.¹⁹ On the Mms6-coated gold surface, aggregates of uniform sized magnetite nanoparticles were also formed, with smaller sizes than those on the ODT surfaces.

Figure 5 shows the influence of two other proteins, m2Mms6 and lysozyme, used as a control coated on the ODT surface. In previous study, both m2Mms6²⁵ and lysozyme²² have been shown to be much less effective as Mms6 in facilitating magnetite nanocrystal formation in the bulk. Here, neither

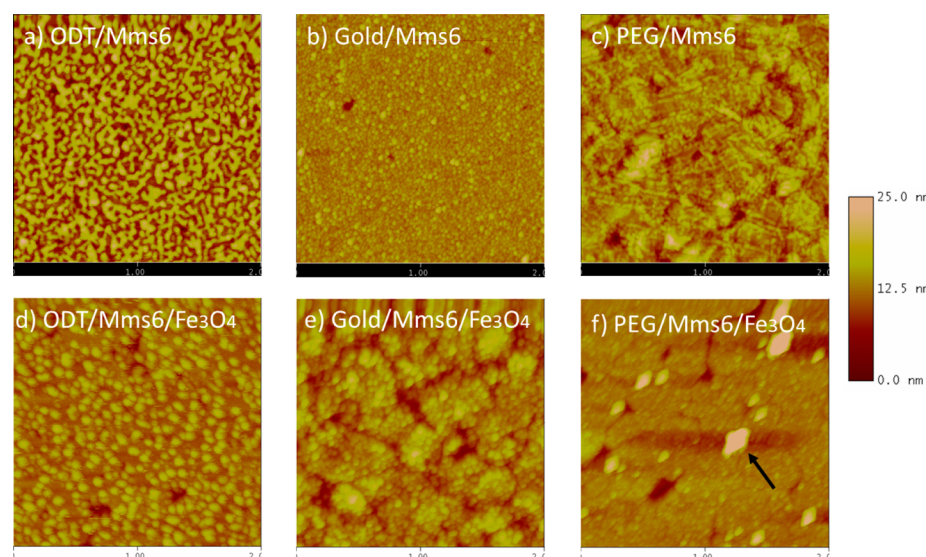


Figure 4. AFM scan of surfaces with Mms6 prior to magnetite nanoparticle synthesis: (a) Mms6 coated ODT, (b) Mms6 coated gold, and (c) Mms6 coated PEG surfaces. After synthesis of magnetite nanoparticles: (d) magnetite grown on Mms6-ODT surface, (e) magnetite grown on Mms6-gold surface, and (f) magnetite grown on Mms6-PEG surface. Scan area $2 \mu\text{m} \times 2 \mu\text{m}$.

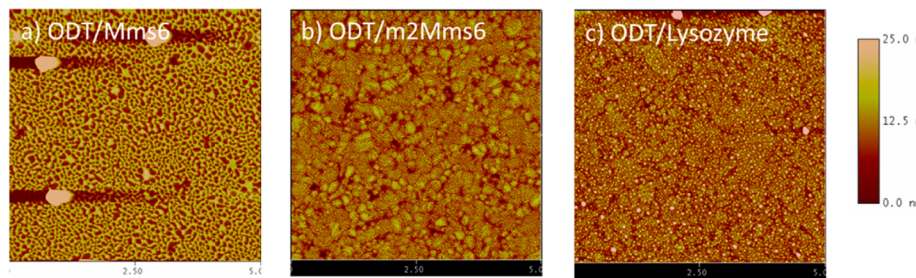


Figure 5. AFM scan of ODT surface with (a) Mms6, (b) m2Mms6, or (c) lysozyme. Scan area $5 \mu\text{m} \times 5 \mu\text{m}$. Only Mms6 can form a “protein network” on the ODT surface, while mutant m2Mms6 or lysozyme cannot, which indicates that the “network” may be important for the formation of magnetite with uniform size.

m2Mms6 nor lysozyme could facilitate the formation of the protein network structure seen with Mms6, which indicated that the type of protein as well as the amino acid sequence is important for the interaction of the protein with the ODT surface. In our previous work,²⁸ we have demonstrated that the ability of Mms6 to self-assemble into a multimeric micelle depends on both N-terminal hydrophobic domain and the C-terminal iron binding domain. Although the C-terminal domain overall is highly charged, it also contains several hydrophobic residues that may be involved in the interaction with N-terminal hydrophobic domain (Leucine128, Leucine132 in the C-terminal domain). Although the intact N-terminal domain still enables the protein to self-assemble into a multimeric complex and interact with the hydrophobic surface (Figure 5b), the structure of the complex formed with the mutant C-terminal is less stable than the wild-type Mms6 complex.²⁸ Only the wild type Mms6 could form a protein network on the ODT surface, suggesting that the Mms6 molecular conformation and especially the arrangement of OH and COOH groups play a critical role in promoting the formation of the protein network. This, in turn, potentially impacts the proteins’ ability to facilitate magnetite nanocrystal formation. This is also consistent with our previous observations of Mms6 self-assembly that is coordinated by both N-terminal and C-terminal domains.²⁸

The chemical states of different surfaces were investigated by XPS. In Figure 6, it shows that there are well-defined spectra for O 1s and N 1s in case of Mms6-ODT surface, as opposed to the ODT surface treated with pure Tris buffer without Mms6. The O 1s spectrum corresponds to oxygen atoms from C=O (531.8 eV) and C=O (533.2 eV) groups, and N 1s spectrum ascribes to nitrogen atoms in C–N (400.3 eV) group. Meanwhile, compared to C 1s spectrum of ODT surface with only one carbon component (C–C/C–H, 284.8 eV), there are two additional moieties in C 1s spectrum of Mms6-ODT surface, which are assigned to carbon atoms from C–O/C–N (285.6 eV) and C=O/N=C=O (288.5 eV) groups. In addition, both ODT and Mms6-ODT surfaces contain low-intensity S 2p peaks. These results confirm the presence of Mms6 protein on the coated ODT surface, since the C–O, C–N, C=O, and N=C=O shown in XPS spectra are all from the Mms6 protein. Figure 7 shows surface characterization of magnetite grown on the ODT surfaces with and without Mms6. On the ODT surface after growing magnetite nanocrystals, the XPS spectra are similar to the pure ODT surface as most of magnetite nanoparticles were washed away during the washing process. On the contrary, on the Mms6-ODT surface, after growing magnetite the C–O, C–N, C=O, and N=C=O components present in XPS spectra support the existence of

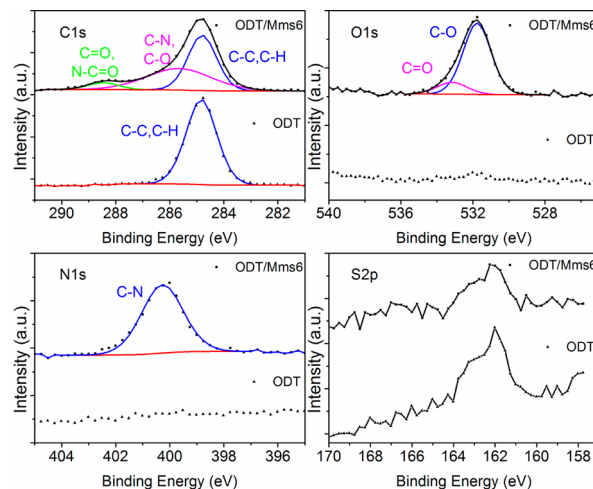


Figure 6. XPS results for ODT/Gold surfaces with (square) and without (triangle) Mms6 protein on them. The surface without Mms6 was still treated with Tris buffer for comparison. Binding energy was calibrated with Au $4f_{7/2}$ (84.0 eV) as a reference.

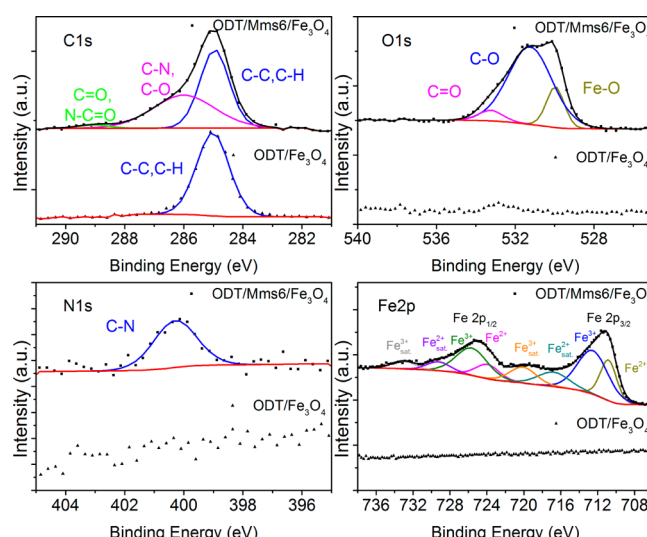


Figure 7. XPS results for the magnetite nanocrystals grown on ODT surfaces, with (square) and without (triangle) Mms6. The surface without Mms6 was still treated with Tris buffer for comparison. Binding energy was calibrated with Au $4f_{7/2}$ (84.0 eV) as a reference.

Mms6 protein and the Fe–O type moiety (530.0 eV) in the O 1s spectrum and the extra Fe 2p peaks indicate formation of magnetite nanocrystals on Mms6-ODT surface. The Fe 2p

spectrum with two constituent peaks ($\text{Fe } 2\text{p}_{1/2}$ and $\text{Fe } 2\text{p}_{3/2}$), and their satellites can be deconvoluted into components (Fe^{2+} $2\text{p}_{3/2}$, 710.8 eV; Fe^{3+} $2\text{p}_{3/2}$, 712.5 eV; Fe^{2+} $2\text{p}_{1/2}$, 723.9 eV; and Fe^{3+} $2\text{p}_{1/2}$, 725.6 eV) ascribed to Fe^{3+} and Fe^{2+} ions from magnetite.^{42,43} Therefore, the XPS results confirm that Mms6 was present on the ODT surface and could promote magnetite formation, which is consistent with the AFM observations.

SEM was used to visualize the magnetite nanoparticles grown on ODT and gold surfaces with and without Mms6 (Figure 8)

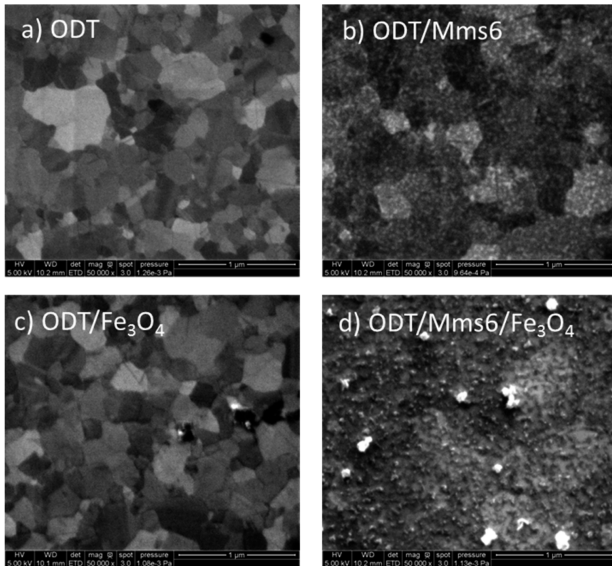


Figure 8. SEM secondary electron images of (a) ODT surface, (b) Mms6-coated ODT surface, (c) magnetite grown on ODT surface, and (d) magnetite grown on Mms6-coated ODT surface.

and 9). On ODT surfaces, nothing could be seen except crystal grains from polycrystalline gold underneath the ODT monolayer (Figure 8a). No clear information from surface topography and morphology could be observed in this secondary electron image, while crystallographic contrast of gold grains due to the effect of electron channeling⁴⁴ was shown, which verified that the surface was very flat. Mms6 coating on ODT surfaces clearly increased the surface roughness uniformly (Figure 8b) resulting from formation of protein network. After magnetite nanocrystals were grown on the ODT surface and Mms6-ODT surface, bright nanoparticles were found attached to the surface. Without ODT, the Mms6 coated gold surface looked flat (Figure 9a and b) compared to Mms6-ODT surface (Figure 8b), probably because the very small roughness of Mms6 on gold shown in AFM is beyond the detection limit of SEM. Nanoparticles on the Mms6-coated gold surface formed very large aggregates (up to 2 μm) and were distributed on the surface without any order (Figure 9c and d). All the bright particles had strong Fe and O signals in energy-dispersive X-ray spectroscopy (EDS) spectrum (Figure S3), suggesting that they are magnetite nanoparticles. Compared with surfaces without ODT, only a few magnetite nanoparticles were left on the ODT surface after washing (Figure 8c), while a large number of fine magnetite nanoparticles including some small aggregates uniformly covered the Mms6-ODT surface (Figure 8d and 9e and f), which is consistent with AFM results. Figure 9e shows the uniform distribution of magnetite nanoparticles on Mms6-

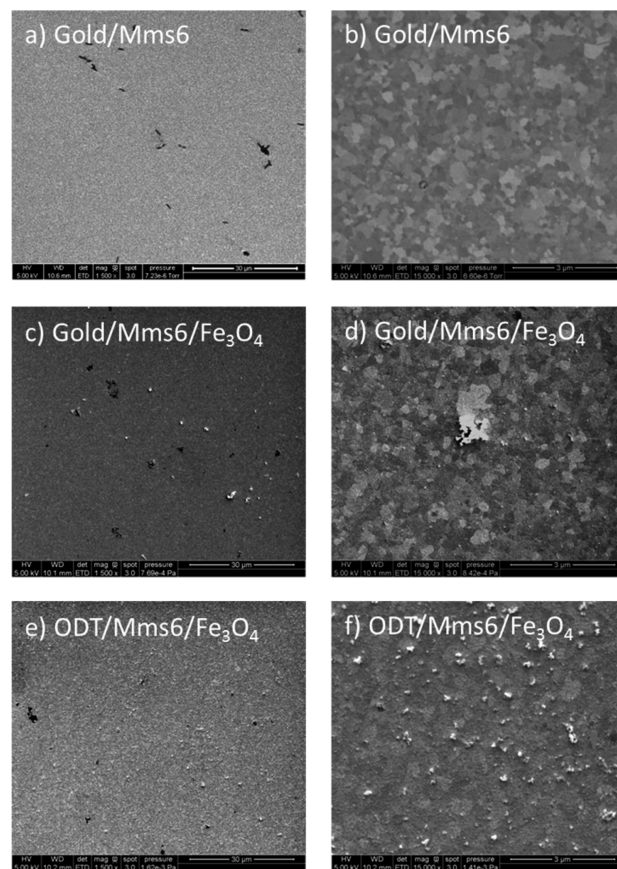


Figure 9. SEM secondary electron images with different magnifications of (a and b) Mms6-coated gold surface, (c and d) magnetite grown on Mms6-coated gold surface, (e and f) magnetite grown on Mms6-coated ODT surface.

ODT surface on a much larger scale than could be observed by AFM.

MFM was used to measure the magnetic response of the magnetite nanoparticles on the surfaces. If there is contrast in the MFM scan, it supports the presence of magnetic materials on the surface. Areas with excess amounts of magnetite nanoparticles were scanned. Therefore, if the MFM image had the same pattern as the AFM image, it may be due to the excess height of the surface and not due to the magnetic response. In Figure S4, only the magnetite nanoparticles grown on the ODT surface show a different contrast pattern on the MFM image than the AFM image, which could be an indication of a stronger magnetic response in that case due to more well-formed nanocrystals.

In summary, it was found that Mms6 can form a protein network on the hydrophobic ODT coated surface, and then promote the formation of magnetite nanoparticles of uniform sizes similar to those seen in nature. The ability of Mms6 to form a network on hydrophobic surfaces such as ODT may be due to its amphiphilic property and its demonstrated ability to incorporate into a hydrophobic lipid bilayers of liposomes.²⁵ The significant decrease in the contact angle of ODT surface after Mms6 coating (Figure 3) suggests that the proteins align on the hydrophobic surface with hydrophilic C-terminal domains on the top. Here we also show that the network-like structure of Mms6 functions *in vitro* in such a hydrophobic environment. Our previous study has indicated that, in bulk solution Mms6 micelles interact with iron ions and prefer to

form 2D disk-like or 3D mass-fractal-like aggregates with large surface area, which may contribute to formation of large magnetite nanocrystals.²⁶ In this study, the ODT monolayer seems to allow Mms6 to self-assemble into a protein network that also provide a large surface area for iron binding, which, in turn, enables the formation of magnetic nanoparticles. The C-terminal domain of Mms6 is known to be necessary for promoting the magnetite formation, and mutants, such as m2Mms6, with changes to the C-terminal domain sequence, no longer promote magnetite formation effectively.^{22,25} Based on the results of this study, we propose that the hydrophobic N-terminal domain of Mms6 embeds in the hydrophobic ODT surfaces, forming a protein network structure. It is worth noting that Mms6 is amphiphilic and self-assembles to multimeric micelles in bulk solution,^{25,26} and these micelles have been shown to exist in solution under constant equilibrium with the unimeric proteins by FPLC analysis of both wild-type and two mutants of Mms6.²⁸ The hydrophobic interaction between N-terminal domain of Mms6 and the ODT surface consumes free unimers in solution and changes the original equilibrium state to provide more unimers, which results in coating of Mms6 on ODT surface after incubation. The Mms6 gene translation product is predicted as a transmembrane protein and the transmembrane helix contains only hydrophobic residues.⁴⁵ The ODT surface may create conditions for the protein that are more similar to its native lipid bilayer environment of magnetosome membrane, thus facilitating the formation of uniformly sized and more well-defined magnetite nanoparticles,⁴⁶ similar to those seen in nature.

CONCLUSIONS

We investigated Mms6 for its function of promoting magnetite nanocrystal formation on surfaces with different hydrophobicities. It was found that Mms6 on hydrophobic ODT monolayer on gold substrates could form a protein network structure that displayed better functionality in promoting the formation of uniformly sized magnetite nanoparticles on the surface. On the contrary, hydrophilic PEG surfaces exhibited protein resistance. Furthermore, Mms6 micelles adsorbed on bare gold surfaces without forming a protein network structure. Compared to magnetite grown on the Mms6-coated ODT surfaces, the magnetite nanocrystals formed on PEG and gold surfaces were smaller and less magnetic, and more easily washed away. Mms6 is believed to be a membrane protein *in vivo*, and we propose that the N-terminal domain of Mms6 interacts mainly through hydrophobic forces with the ODT surface in a way similar to Mms6 situated in the membrane *in vivo* and the C-terminal domain facilitates growth of magnetite nanocrystals. Our results have also shown that Mms6 immobilized on surface by hydrophobic interaction can be used as a template for specific magnetite biominerization on surfaces, which provides an effective and cheap bottom-up approach to fabricating magnetic devices with magnetite, cobalt doped magnetite⁴⁷ or cobalt ferrite³² nanoparticles on surfaces at room temperature without using harsh chemicals. Moreover, the system in this study is very flexible and Mms6 can be exploited for surface magnetic nanomaterials synthesis, in which functionalized surfaces or patterned surfaces can be used as substrates for synthesis. These surfaces, with site-specifically fabricated magnetic nanocrystals, can be further applied to the development of sensors or data storage devices. The work also provides a facile way to control the bioinspired synthesis by tailoring the hydrophobicity of the surfaces.

ASSOCIATED CONTENT

Supporting Information

The Supporting Information is available free of charge on the ACS Publications website at DOI: 10.1021/acs.iecr.5b01413.

AFM images, XRD pattern, EDS plots, and MFM scans (PDF)

AUTHOR INFORMATION

Corresponding Author

*E-mail: suryakm@iastate.edu.

Notes

The authors declare no competing financial interest.

^aX.L. and H.Z. are joint first authors.

ACKNOWLEDGMENTS

S.K.M. is grateful for the inspiration provided by Prof. Doraiswami Ramkrishna through his outstanding body of work and through his graduate teaching at Purdue that directly impacted her. We thank Pierre Palo from M.N.-H.'s group at Ames Laboratory for preparing the Mms6 protein preparations. Research at Ames Laboratory was supported by the U.S. Department of Energy, Office of the Basic Energy Sciences, Division of Materials Sciences and Engineering. Ames Laboratory is operated for the U.S. Department of Energy by Iowa State University under Contract Number DE-AC02-07CH11358. The use of Magnetic Force Microscopy at the Argonne National Laboratory was supported by the U.S. Department of Energy under Contract Number DE-AC02-06CH11357.

REFERENCES

- (1) Lu, A.-H.; Salabas, E. L.; Schüth, F. Magnetic Nanoparticles: Synthesis, Protection, Functionalization, and Application. *Angew. Chem., Int. Ed.* **2007**, *46*, 1222–1244.
- (2) Jeong, U.; Teng, X.; Wang, Y.; Yang, H.; Xia, Y. Superparamagnetic Colloids: Controlled Synthesis and Niche Applications. *Adv. Mater.* **2007**, *19*, 33–60.
- (3) Gao, J.; Gu, H.; Xu, B. Multifunctional Magnetic Nanoparticles: Design, Synthesis, and Biomedical Applications. *Acc. Chem. Res.* **2009**, *42*, 1097–1107.
- (4) Hao, R.; Xing, R.; Xu, Z.; Hou, Y.; Gao, S.; Sun, S. Synthesis, Functionalization, and Biomedical Applications of Multifunctional Magnetic Nanoparticles. *Adv. Mater.* **2010**, *22*, 2729–2742.
- (5) Tartaj, P.; Morales, M. d. P.; Veintemillas-Verdaguer, S.; González-Carreño, T.; Serna, C. J. The preparation of magnetic nanoparticles for applications in biomedicine. *J. Phys. D: Appl. Phys.* **2003**, *36*, R182.
- (6) Park, J.; An, K.; Hwang, Y.; Park, J.-G.; Noh, H.-J.; Kim, J.-Y.; Park, J.-H.; Hwang, N.-M.; Hyeon, T. Ultra-large-scale syntheses of monodisperse nanocrystals. *Nat. Mater.* **2004**, *3*, 891–895.
- (7) Sun, S.; Zeng, H. Size-Controlled Synthesis of Magnetite Nanoparticles. *J. Am. Chem. Soc.* **2002**, *124*, 8204–8205.
- (8) Laurent, S.; Forge, D.; Port, M.; Roch, A.; Robic, C.; Vander Elst, L.; Muller, R. N. Magnetic Iron Oxide Nanoparticles: Synthesis, Stabilization, Vectorization, Physicochemical Characterizations, and Biological Applications. *Chem. Rev.* **2008**, *108*, 2064–2110.
- (9) Bazylinski, D. A.; Frankel, R. B. Magnetosome formation in prokaryotes. *Nat. Rev. Microbiol.* **2004**, *2*, 217–230.
- (10) Jimenez-Lopez, C.; Romanek, C. S.; Bazylinski, D. A. Magnetite as a prokaryotic biomarker: A review. *J. Geophys. Res.* **2010**, *115*, G00G03.
- (11) Siponen, M. I.; Legrand, P.; Widdrat, M.; Jones, S. R.; Zhang, W.-J.; Chang, M. C. Y.; Faivre, D.; Arnoux, P.; Pignol, D. Structural insight into magnetochrome-mediated magnetite biominerization. *Nature* **2013**, *502*, 681–684.

- (12) Mann, S.; Sparks, N. H. C.; Frankel, R. B.; Bazylinski, D. A.; Jannasch, H. W. Biominerization of ferrimagnetic greigite (Fe_3S_4) and iron pyrite (FeS_2) in a magnetotactic bacterium. *Nature* **1990**, *343*, 258–261.
- (13) Lu, Y.; Dong, L.; Zhang, L.-C.; Su, Y.-D.; Yu, S.-H. Biogenic and biomimetic magnetic nanosized assemblies. *Nano Today* **2012**, *7*, 297–315.
- (14) Fdez-Gubieda, M. L.; Muela, A.; Alonso, J.; García-Prieto, A.; Olivi, L.; Fernández-Pacheco, R.; Barandiarán, J. M. Magnetic Biominerization in Magnetospirillum gryphiswaldense: Time-Resolved Magnetic and Structural Studies. *ACS Nano* **2013**, *7*, 3297–3305.
- (15) Lefèvre, C. T.; Menguy, N.; Abreu, F.; Lins, U.; Pósfai, M.; Prozorov, T.; Pignol, D.; Frankel, R. B.; Bazylinski, D. A. A Cultured Greigite-Producing Magnetotactic Bacterium in a Novel Group of Sulfate-Reducing Bacteria. *Science* **2011**, *334*, 1720–1723.
- (16) Komeili, A. Molecular Mechanisms of Magnetosome Formation. *Annu. Rev. Biochem.* **2007**, *76*, 351–366.
- (17) Fratzl, P.; Weinkamer, R. Nature's hierarchical materials. *Prog. Mater. Sci.* **2007**, *52*, 1263–1334.
- (18) Cölfen, H.; Mann, S. Higher-Order Organization by Mesoscale Self-Assembly and Transformation of Hybrid Nanostructures. *Angew. Chem., Int. Ed.* **2003**, *42*, 2350–2365.
- (19) Prozorov, T.; Bazylinski, D. A.; Mallapragada, S. K.; Prozorov, R. Novel magnetic nanomaterials inspired by magnetotactic bacteria: Topical review. *Mater. Sci. Eng., R* **2013**, *74*, 133–172.
- (20) Kolinko, I.; Lohsse, A.; Borg, S.; Raschdorf, O.; Jogler, C.; Tu, Q.; Pósfai, M.; Tompa, E.; Plitzko, J. M.; Brachmann, A.; Wanner, G.; Müller, R.; Zhang, Y.; Schuler, D. Biosynthesis of magnetic nanostructures in a foreign organism by transfer of bacterial magnetosome gene clusters. *Nat. Nanotechnol.* **2014**, *9*, 193–197.
- (21) Arakaki, A.; Webb, J.; Matsunaga, T. A novel protein tightly bound to bacterial magnetic particles in Magnetospirillum magneticum strain AMB-1. *J. Biol. Chem.* **2003**, *278*, 8745–8750.
- (22) Prozorov, T.; Mallapragada, S. K.; Narasimhan, B.; Wang, L.; Palo, P.; Nilsen-Hamilton, M.; Williams, T. J.; Bazylinski, D. A.; Prozorov, R.; Canfield, P. C. Protein-Mediated Synthesis of Uniform Superparamagnetic Magnetite Nanocrystals. *Adv. Funct. Mater.* **2007**, *17*, 951–957.
- (23) Amemiya, Y.; Arakaki, A.; Staniland, S. S.; Tanaka, T.; Matsunaga, T. Controlled formation of magnetite crystal by partial oxidation of ferrous hydroxide in the presence of recombinant magnetotactic bacterial protein Mms6. *Biomaterials* **2007**, *28*, 5381–5389.
- (24) Arakaki, A.; Masuda, F.; Amemiya, Y.; Tanaka, T.; Matsunaga, T. Control of the morphology and size of magnetite particles with peptides mimicking the Mms6 protein from magnetotactic bacteria. *J. Colloid Interface Sci.* **2010**, *343*, 65–70.
- (25) Wang, L.; Prozorov, T.; Palo, P. E.; Liu, X.; Vaknin, D.; Prozorov, R.; Mallapragada, S.; Nilsen-Hamilton, M. Self-Assembly and Biphasic Iron-Binding Characteristics of Mms6, A Bacterial Protein That Promotes the Formation of Superparamagnetic Magnetite Nanoparticles of Uniform Size and Shape. *Biomacromolecules* **2012**, *13*, 98–105.
- (26) Zhang, H.; Liu, X.; Feng, S.; Wang, W.; Schmidt-Rohr, K.; Akinc, M.; Nilsen-Hamilton, M.; Vaknin, D.; Mallapragada, S. Morphological Transformations in the Magnetite Biomineralizing Protein Mms6 in Iron Solutions: A Small-Angle X-ray Scattering Study. *Langmuir* **2015**, *31*, 2818–2825.
- (27) Wang, W.; Bu, W.; Wang, L.; Palo, P. E.; Mallapragada, S.; Nilsen-Hamilton, M.; Vaknin, D. Interfacial Properties and Iron Binding to Bacterial Proteins That Promote the Growth of Magnetite Nanocrystals: X-ray Reflectivity and Surface Spectroscopy Studies. *Langmuir* **2012**, *28*, 4274–4282.
- (28) Feng, S.; Wang, L.; Palo, P.; Liu, X.; Mallapragada, S.; Nilsen-Hamilton, M. Integrated self-assembly of the mms6 magnetosome protein to form an iron-responsive structure. *Int. J. Mol. Sci.* **2013**, *14*, 14594–14606.
- (29) Arakaki, A.; Masuda, F.; Matsunaga, T. Iron oxide crystal formation on a substrate modified with the Mms6 protein from magnetotactic bacteria. *MRS Online Proc. Libr.* **2009**, DOI: [10.1557/proc-1187-KK03-08](https://doi.org/10.1557/proc-1187-KK03-08).
- (30) Galloway, J. M.; Bramble, J. P.; Rawlings, A. E.; Burnell, G.; Evans, S. D.; Staniland, S. S. Biotemplated Magnetic Nanoparticle Arrays. *Small* **2012**, *8*, 204–208.
- (31) Galloway, J. M.; Bramble, J. P.; Rawlings, A. E.; Burnell, G.; Evans, S. D.; Staniland, S. S. Nanomagnetic arrays formed with the biominerization protein Mms6. *J. Nano Res.* **2012**, *17*, 127–146.
- (32) Prozorov, T.; Palo, P.; Wang, L.; Nilsen-Hamilton, M.; Jones, D.; Orr, D.; Mallapragada, S. K.; Narasimhan, B.; Canfield, P. C.; Prozorov, R. Cobalt Ferrite Nanocrystals: Out-Performing Magnetotactic Bacteria. *ACS Nano* **2007**, *1*, 228–233.
- (33) Hegner, M.; Wagner, P.; Semenza, G. Ultralarge atomically flat template-stripped Au surfaces for scanning probe microscopy. *Surf. Sci.* **1993**, *291*, 39–46.
- (34) Bain, C. D.; Troughton, E. B.; Tao, Y. T.; Evall, J.; Whitesides, G. M.; Nuzzo, R. G. Formation of monolayer films by the spontaneous assembly of organic thiols from solution onto gold. *J. Am. Chem. Soc.* **1989**, *111*, 321–335.
- (35) Cerruti, M.; Fissolo, S.; Carraro, C.; Ricciardi, C.; Majumdar, A.; Maboudian, R. Poly(ethylene glycol) Monolayer Formation and Stability on Gold and Silicon Nitride Substrates. *Langmuir* **2008**, *24*, 10646–10653.
- (36) Harder, P.; Grunze, M.; Dahint, R.; Whitesides, G. M.; Laibinis, P. E. Molecular Conformation in Oligo(ethylene glycol)-Terminated Self-Assembled Monolayers on Gold and Silver Surfaces Determines Their Ability To Resist Protein Adsorption. *J. Phys. Chem. B* **1998**, *102*, 426–436.
- (37) Lukanathan, A. R.; Zhang, S.; Regina, V. R.; Cole, M. A.; Ogaki, R.; Dong, M.; Besenbacher, F.; Meyer, R. L.; Kingshott, P. Mixed poly(ethylene glycol) and oligo(ethylene glycol) layers on gold as nonfouling surfaces created by backfilling. *Biointerphases* **2011**, *6*, 180–188.
- (38) Unsworth, L. D.; Tun, Z.; Sheardown, H.; Brash, J. L. Chemisorption of thiolated poly(ethylene oxide) to gold: surface chain densities measured by ellipsometry and neutron reflectometry. *J. Colloid Interface Sci.* **2005**, *281*, 112–121.
- (39) Pfeiffer, C.; Rehbock, C.; Hühn, D.; Carrillo-Carrion, C.; de Aberasturi, D. J.; Merk, V.; Barcikowski, S.; Parak, W. J. Interaction of colloidal nanoparticles with their local environment: the (ionic) nanoenvironment around nanoparticles is different from bulk and determines the physico-chemical properties of the nanoparticles. *J. R. Soc., Interface* **2014**, *11*, 20130931.
- (40) Illés, E.; Tombácz, E. The effect of humic acid adsorption on pH-dependent surface charging and aggregation of magnetite nanoparticles. *J. Colloid Interface Sci.* **2006**, *295*, 115–123.
- (41) Harris, J. M. *Poly(Ethylene Glycol) Chemistry: Biotechnical and Biomedical Applications*; Plenum Press: New York, 1992.
- (42) Bhargava, G.; Gouzman, I.; Chun, C. M.; Ramanarayanan, T. A.; Bernasek, S. L. Characterization of the “native” surface thin film on pure polycrystalline iron: A high resolution XPS and TEM study. *Appl. Surf. Sci.* **2007**, *253*, 4322–4329.
- (43) Nan, A.; Turcu, R.; Liebscher, J. Magnetite-polylactic acid core-shell nanoparticles by ring-opening polymerization under microwave irradiation. *J. Polym. Sci., Part A: Polym. Chem.* **2012**, *50*, 1485–1490.
- (44) LLOYD, G. Atomic number and crystallographic contrast images with the SEM: a review of backscattered electron techniques. *Mineral. Mag.* **1987**, *51*, 3–19.
- (45) Nudelman, H.; Zarivach, R. Structure prediction of magnetosome-associated proteins. *Front. Microbiol.* **2014**, DOI: [10.3389/fmicb.2014.00009](https://doi.org/10.3389/fmicb.2014.00009).
- (46) Rahn-Lee, L.; Komeili, A. The Magnetosome Model: Insights into the Mechanisms of Bacterial Biominerization. *Front. Microbiol.* **2013**, DOI: [10.3389/fmicb.2013.00352](https://doi.org/10.3389/fmicb.2013.00352).
- (47) Galloway, J. M.; Arakaki, A.; Masuda, F.; Tanaka, T.; Matsunaga, T.; Staniland, S. S. Magnetic bacterial protein Mms6 controls

morphology, crystallinity and magnetism of cobalt-doped magnetite nanoparticles in vitro. *J. Mater. Chem.* **2011**, *21*, 15244–15254.